



**HAL**  
open science

## Contactless AF-SIW phase shifters based on periodic structures at mmWaves

Cleofás Segura-Gómez, Mario Pérez-Escribano, Andrés Biedma-Pérez, Ángel Palomares-Caballero, Pablo Padilla

► **To cite this version:**

Cleofás Segura-Gómez, Mario Pérez-Escribano, Andrés Biedma-Pérez, Ángel Palomares-Caballero, Pablo Padilla. Contactless AF-SIW phase shifters based on periodic structures at mmWaves. *AEÜ - International Journal of Electronics and Communications / Archiv für Elektronik und Übertragungstechnik*, 2024, pp.155320. 10.1016/j.aeue.2024.155320 . hal-04575543

**HAL Id: hal-04575543**

**<https://hal.science/hal-04575543v1>**

Submitted on 15 May 2024

**HAL** is a multi-disciplinary open access archive for the deposit and dissemination of scientific research documents, whether they are published or not. The documents may come from teaching and research institutions in France or abroad, or from public or private research centers.

L'archive ouverte pluridisciplinaire **HAL**, est destinée au dépôt et à la diffusion de documents scientifiques de niveau recherche, publiés ou non, émanant des établissements d'enseignement et de recherche français ou étrangers, des laboratoires publics ou privés.

## Highlights

### **Contactless AF-SIW Phase Shifters Based on Periodic Structures at mmWaves**

Cleofás Segura-Gómez, Mario Pérez-Escribano, Andrés Biedma-Pérez, Ángel Palomares-Caballero, Pablo Padilla

- We propose a design method to achieve waveguide phase shifters in CLAF-SIW technology at the millimeter-wave frequency range.
- Different phase shift behaviors for new application-specific requirements are obtained through different types of SIH unit cells.
- The proof of concept is demonstrated using several prototypes consisting of a set of phase shifters.
- Good agreement is obtained between measurements and simulations.

# Contactless AF-SIW Phase Shifters Based on Periodic Structures at mmWaves

Cleofás Segura-Gómez<sup>a</sup>, Mario Pérez-Escribano<sup>a,b,\*</sup>, Andrés Biedma-Pérez<sup>a</sup>,  
Ángel Palomares-Caballero<sup>c</sup> and Pablo Padilla<sup>a</sup>

<sup>a</sup>Department of Signal Theory, Telematics and Communications, Centre for Information and Communication Technologies (CITIC-UGR), University of Granada, Calle Periodista Rafael Gómez Montero, 2, Granada, 18071, Spain

<sup>b</sup>Telecommunication Research Institute (TELMA), Universidad de Málaga, E.T.S. Ingeniería de Telecomunicación, Boulevard Louis Pasteur, 35, Málaga, 29010, Málaga, Spain

<sup>c</sup>Institut d'Electronique et des Technologies du numérique (IETR), UMR CNRS 6164, INSA Rennes,, Rennes, 35700, France

## ARTICLE INFO

### Keywords:

Contactless air-filled SIW technology  
electromagnetic band gap (EBG)  
glide symmetry  
periodic structure  
phase shifter  
printed circuit board (PCB) technology.

## ABSTRACT

This document presents different phase shifter designs implemented in contactless air-filled substrate-integrated waveguide (CLAF-SIW) technology. The phase shifters are based on unit cells that avoid leakage losses in the assembled layers and produce the desired phase shift along the waveguide. The unit cells are represented by waveguides whose lateral walls have double-mushroom structures, and phase-shifting elements are in their propagation zone. The proposed phase-shifting elements are integrated cavities, integrated cavities with patches, and integrated cavities with mushroom-like patches. Transitions are needed to match impedances between the waveguides loaded with phase-shifting elements and a reference CLAF-SIW. Other transitions are designed to measure the prototypes, from coplanar waveguide to SIW and SIW to CLAF-SIW. Finally, some prototypes are manufactured to provide an experimental validation of the proposed phase-shifting elements. Good agreement is obtained between the simulated and measured results for all the CLAF-SIW phase shifters in the frequency range between 30 and 50 GHz.

## 1. Introduction

Planar technologies are becoming a powerful tool for designing new communications systems due to their ease of integration and cost [1]. The introduction of the waveguide in the substrate, also called substrate integrated waveguide (SIW), has enabled an alternative to the conventional waveguide for the millimeter-wave frequency range [2, 3].

Nevertheless, in contrast to other waveguide technologies employed in the millimeter-wave range, such as gap-waveguide (GW) technologies [4], insertion losses in the dielectric become impractical. Therefore, in an attempt to maintain the advantages of SIW while reducing losses, alternatives such as air-filled SIW (AF-SIW) [5] or empty SIW (E-SIW) [6] have emerged. In AF-SIW technology, the electromagnetic (EM) waves propagate in an air zone resulting from removing the dielectric part of the laminate. The lateral rows of metallic vias are used in SIW technology to achieve the waveguide conditions. Two extra bottom and top metal layers are necessary to ensure these conditions. However, the multilayer configuration of this waveguide technology becomes vulnerable to losses, such as the field leakage in the tiny air gaps between the layers due to manufacturing tolerance and the assembly (from now on referred

to as “tolerance gaps”). Contactless techniques, such as those employed in conventional GW technologies, can also avoid this undesirable effect. These technologies generally include electromagnetic band-gap (EBG) structures in the lateral zones of the waveguide [7, 8]. For example, in [9], a metasurface composed of periodic double mushroom-like patches (from now on referred to simply as “mushrooms”), which produces an artificial magnetic conductor (AMC) boundary conditions, are combined with the bottom and top metallic layers to generate the EBG unit cells. This new alternative to SIW technology is called contactless air-filled SIW (CLAF-SIW).

Numerous components have been designed in SIW technology [10], in AF-SIW technology [11, 12] and in E-SIW technology [13, 14]. However, CLAF-SIW technology has yet to be extensively exploited for radio frequency (RF) use. A direct RF application is the design of a phase shifter. Examples of phase-shifting elements in other waveguide technologies at millimeter waves can be found in the literature [15]. The phase-shifting elements in the referenced work are periodic holes in the propagation zone of a GW. These elements are difficult to be introduced in printed circuit board (PCB) technology. Nonetheless, a unit cell based on PCB that tunes the refractive index for a lens application is described in [16] through substrate-integrated holes (SIH). This method allows the introduction of integrated phase-shifting elements in a parallel-plate waveguide that perturb the propagation of the EM waves. There are other alternatives to the use of phase-shifting unit cells, such as the ones based on the introduction of dielectric material, either on

\*Corresponding author

 cleofas@ugr.es (C. Segura-Gómez); mpe@ic.uma.es (M.

Pérez-Escribano); abieper@ugr.es (A. Biedma-Pérez);

Angel.Palomares-Caballero2@insa-rennes.fr (Á. Palomares-Caballero);

pablopadilla@ugr.es (P. Padilla)

ORCID(s): 0000-0002-9347-287X (C. Segura-Gómez);

0000-0003-4618-8363 (M. Pérez-Escribano); 0000-0003-1387-7250 (A.

Biedma-Pérez); 0000-0002-3999-3236 (Á. Palomares-Caballero);

0000-0002-4874-6106 (P. Padilla)

both sides of the waveguide [11] or in the center of the waveguide [12].

This paper proposes a set of phase shifter designs in CLAF-SIW technology with different performances, focusing on constant phase shift over a wide bandwidth and in the interest of phase compensation in certain devices with frequency-changing behavior [17]. A preliminary study of the phase-shifting elements used is in [18], but in the present work, they are implemented as SIH with experimental validation.

## 2. Phase shifter design

This section details the complete design of the phase shifters, showing the effects of a basic CLAF-SIW, the different transitions required, and the elements that allow modification of the phase constant ( $\beta$ ). For the design, the laminate used is RO4003C laminate, which has a relative permittivity of substrate  $\epsilon_r$ , of 3.55 and a loss tangent  $\tan\delta$  of 0.0027 at 10 GHz. The thickness used for the external layers is 0.813 mm (large thickness produces undesirable effects in the SIH [19]), and the thickness of the middle layer is 0.508 mm. The cladding, made of copper, in all the layers is  $35\ \mu\text{m}$ . The full-wave electromagnetic software used is CST Studio Suite.

### 2.1. Analysis of the CLAF-SIW structure

In planar technologies, mushroom unit cells are often used to achieve AMC surfaces [20]. The mushroom comprises a metallic patch over a substrate connected to the ground by a via. In the case of CLAF-SIW, where it is intended to avoid two tolerance gaps, there exists a unit cell with a lower and an upper patch, known as double mushroom [21]. This EBG unit cell is illustrated in Fig. 1(a). The stopband can be adjusted by modifying parameters such as the periodicity between the unit cells, the via diameter, and the patch size. Specifically, the lower modes are the most affected by the patch size and the gap size because they propagate there. On the other hand, the higher modes propagating through the dielectric are more affected by the metallic via and the periodicity. The unit cell is designed to avoid electromagnetic field leakage approximately between 30 GHz to 50 GHz for two 0.1 mm tolerance gaps (as the worst situation), as shown in Fig. 1(b). Consequently, the operating frequency range of the CLAF-SIW is determined by this frequency range.

Using rows of three double-mushroom unit cells on each lateral side of the CLAF-SIW ensures the confinement of the EM field in the waveguide and avoids leakage losses. Fig. 2(a) shows a unit cell composed by double-mushrooms at both sides of the waveguide to create a reference CLAF-SIW. It should be noted that there is some slight modification between the double mushroom unit cell used to calculate the stopband (see Fig. 1(a)) and the final EBG unit cell (see Fig. 2(a)). The latter unit cell uses a structure inherited from [18], where the double mushroom via is displaced to one side. This does not modify the frequency behavior of the stopband and generates certain advantages. It allows the reduction

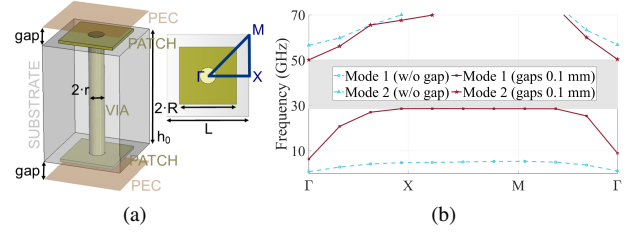


**Figure 1:** EBG structure design: (a) Unit cell design, and (b) Dispersion diagram. The stopband is highlighted in gray. The dimensions (in mm) are:  $R = 0.6$ ,  $L = 1.3$ ,  $r = 0.2$ ,  $h_0 = 0.508$ .

of the size of the mushrooms [22] and also reduces the percentage of dielectric remaining between the via and the air zone of the waveguide in CLAF-SIW. Since there is a dielectric area at both sides of the propagation zone in CLAF-SIW and AF-SIW, it can be considered a partially loaded waveguide [23]. Thus, it may be a problem to compute accurately the cut-off frequency and the amount of dielectric losses [5]. In Fig. 2(b), different E-field distributions in the transversal plane (XY plane) of CLAF-SIW are displayed. The behavior in our frequency range is similar to that of traditional waveguides containing a single mode, in this case, quasi- $\text{TE}_{10}$ . The E-field distributions exemplify situations of CLAF-SIW without gap, with gap and no EBG unit cells on the lateral sides (case of AF-SIW with a gap). A leakage is checked for the AF-SIW case, while the E-field is correctly confined in the waveguide area in CLAF-SIW (both with and without gaps). There is a slight perturbation of the effective width of the propagating mode when tolerance gaps appear or changes its value. This phenomenon is due to modification of the E-field distribution [7]. Fig. 2(c) shows the cut-off frequency of the waveguide composed by Fig. 2(a) and varying gaps. As can be seen, there is an increase in the cut-off frequency with the gap. Thus, a larger gap, as well as lower frequencies, generates worse EBG behavior. In this way, larger gaps force a larger E-field over the lateral row of mushrooms, affecting the possible E-field distribution, and increasing the cut-off frequency.

### 2.2. Phase-shifting elements

Once the CLAF-SIW unit cell has been designed, it is possible to develop waveguide unit cells that allow the modification of the  $\beta$ . In this case, a phase shift is sought by exploiting the propagation zone of the waveguide and the supporting layers. The phase shifters developed in this work are based on periodic unit cells [23], which are designed through modification of the reference CLAF-SIW unit cell. These modifications enable the desired variation of the  $\beta$  (regarding the CLAF-SIW). Because the  $\beta$  of the CLAF-SIW reference is different from the  $\beta$  of the modified CLAF-SIW unit cell, this produces the phase shift per unit cell [24]. To study the phase shift, compare the dispersion diagrams of the unit cell in Fig. 2(a) with the unit cells in Fig. 3. The total phase shift depends on the number of unit cells constituting the phase shifter and the behavior of the  $\beta$  of the unit cell

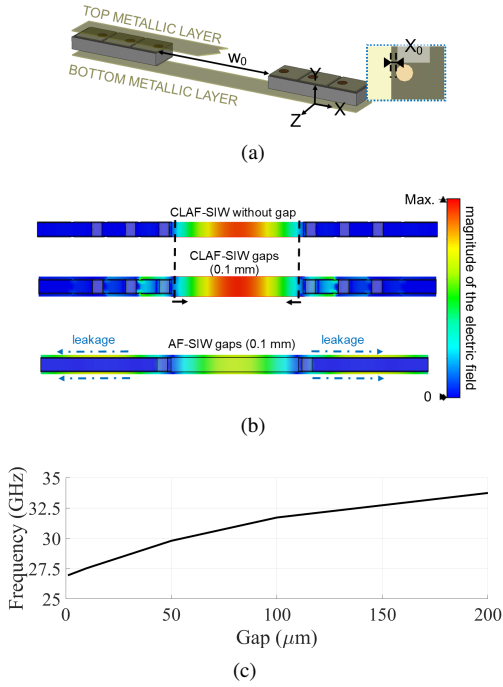


**Figure 2:** CLAF-SIW unit cell: (a) Design, and (b) E-field distribution at the cross-section of a CLAF-SIW without gap, a CLAF-SIW with gaps, and an AF-SIW with gaps (the simulated frequency is 40 GHz). The black solid arrows represent the narrowing of the effective width in the CLAF-SIW. The blue dashed arrows represent the leakage waves in the AF-SIW. (c) Frequency cut-off of the waveguide composed by the unit cell, varying the gaps. Dimensions (in mm):  $w_0 = 5.1$ ,  $h_0 = 0.508$ , and  $X_0 = 0.1$ . The vias of these double mushrooms are displaced to the sides to avoid maximum dielectric between the air and them.

over frequency. Thus, the total phase shift produced will be approximately the product of the phase shift (of the selected unit cell) times the number of concatenated unit cells. For example, if it is desired a phase shifter with a constant phase shift over the frequency, the chosen unit cell must have a  $\beta$  that has a constant difference with the  $\beta$  of the CLAF-SIW over the frequency. In Fig. 3(a), some SIH that are the phase-shifting elements are observed in a CLAF-SIW unit cell. There are three SIHs on the top layer and three on the bottom. The SIH comprises a slot in the cladding and four metallic vias at each side of the hole to confine the EM in the dielectric cavity. The dimensions of the SIH have been selected to be as large as possible to produce the maximum phase-perturbation of the propagating wave and, simultaneously, avoid the excitation of modes inside the SIH and impair performance. The periodicity of these elements modifies the phase shift per unit length; lower periodicities increase the hole size to unit cell length ratio, achieving more compactness, and therefore, this value is selected as low as possible.

As we considered a unit cell in the CLAF-SIW to introduce the phase shift, some symmetries can be applied to this periodic structure through the relative position between

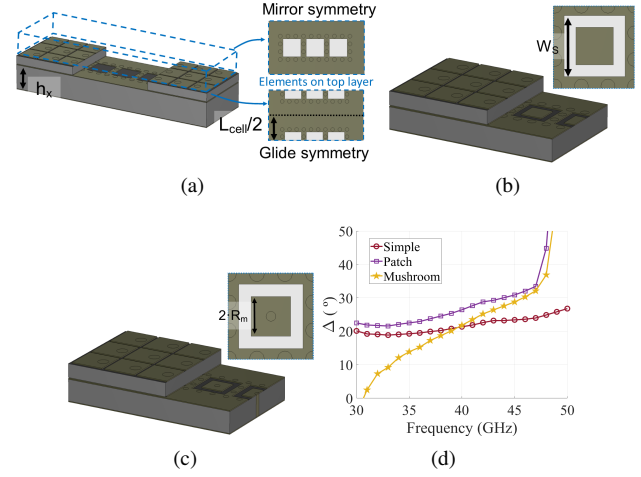


**Figure 3:** Design of phase-shifting unit cells based on SIH: (a) Simple cavity, (b) Cavity and patch, (c) Cavity and mushroom. (d) Phase shift of the SIH unit cells. Dimensions (in mm):  $h_x = 0.813$ ,  $W_s = 1.3$ ,  $R_m = 0.4$ ,  $L_{\text{cell}} = 3.9$ .

upper and lower elements. Fig. 3(a) shows two symmetric configurations for the unit cell, one based on glide symmetry, where the SIH in the upper layer is shifted half of the period regarding the SIH of the bottom layer. The second symmetric configuration is mirror symmetry, where the SIH in the upper layer is precisely above the ones in the bottom. Glide symmetry is demonstrated to eliminate stopbands that can appear when periodic structures are introduced in waveguides [15]. Therefore, the unit cells considered in the design process have a glide-symmetric configuration to take advantage of the abovementioned advantages.

The phase shift provided by simple SIH and SIH with additional elements is analyzed. Fig. 3(d) shows the phase shift between a reference CLAF-SIW unit cell without elements (similar to the one in Fig. 2(a)) and the CLAF-SIW unit cells with phase-shifting elements. The phase shift is calculated by obtaining the difference of the phase constants between the reference waveguide ( $\beta_{ref}$ ) and those loaded with phase-shifting elements ( $\beta_x$ ). The first element is a simple SIH-cavity presented in Fig. 3(a). The dimensions of the SIH are adjusted to achieve the maximum phase shift without frequency dispersion. It is important to note that there is little discrepancy between the phase shift produced for the unit cells based on perfect cavities and the phase shift produced for the unit cells based on SIH. Specifically, the phase shift is slightly higher in SIH unit cells because of the effective width in the cavity due to the vias and the dispersion that occurs at the higher frequencies. The simple SIH unit cell achieves an almost constant phase shift for the considered frequency range. For example at 40 GHz, the phase shift is  $20^\circ$  per unit cell, i.e.  $5.13^\circ/\text{mm}$ . Nine simple SIH unit cells (35.1 mm) would be needed to accomplish a  $180^\circ$  phase shift.

The next phase-shifting element is the patch over the SIH, as is displayed in Fig. 3(b). In this case, the unit cell

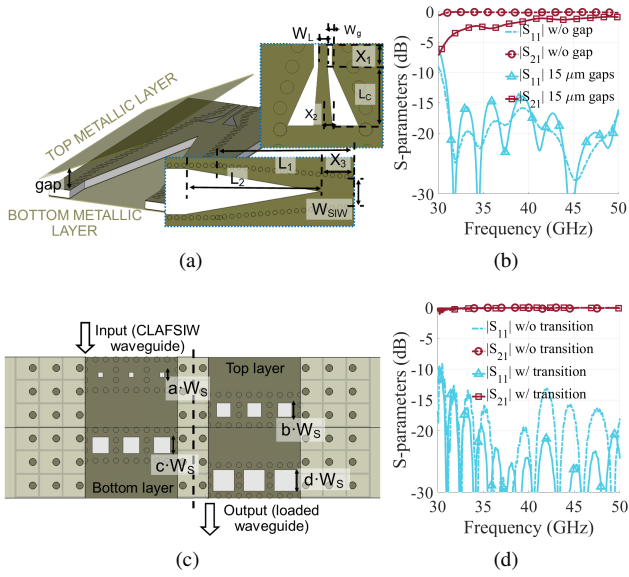


**Figure 4:** Transition from GCPW to AF-SIW: (a) Design, and (b) S-Parameters. Transition from unloaded CLAF-SIW to loaded CLAF-SIW: (c) Design, and (d) S-Parameters. Dimensions (in mm):  $L_C = 2.55$ ,  $W_g = 0.17$ ,  $W_L = 0.35$ ,  $X_1 = 0.55$ ,  $X_2 = 0.35$ ,  $W_L = 3.2$ ,  $L_1 = 18.25$ ,  $L_2 = 15$ ,  $X_3 = 3.75$ ,  $a = 0.2$ ,  $b = 0.6$ ,  $c = 0.7$ ,  $d = 0.9$ .

achieves a higher phase shift over the frequency with a quasi-flat zone and a more linear zone, specifically at the end of the analyzed frequency range (see Fig. 3(d)). Finally, the next phase-shifting element studied is a single mushroom inside the SIH. It is illustrated in Fig. 3(c). The mushroom also produces a linear phase shift over the frequency but with a more significant slope than the previous phase-shifting elements. Observing Fig. 3(d), at lower frequencies, the mushroom provides a lower phase shift regarding the simple SIH and patch but a higher phase shift when the end of the range is considered. The different phase shifts occurring in the modified unit cells are due to the resonances included with the additional elements (patches and mushrooms). A slope of  $1.49^\circ/\text{GHz}$  is recorded in the range between 35 GHz and 45 GHz (while the slope of the first cell type is  $0.42^\circ/\text{GHz}$  and of the second is  $0.84^\circ/\text{GHz}$  in the same frequency range). This type of modified unit cells allows adaptation to new phase shift requirements for new applications [17] other than constant phase shift over large bandwidths.

### 2.3. Transitions

In this work, the goal is the design of several phase shifter designs by concatenating the above unit cells based on CLAF-SIW and SIH. As a proof of concept, the length of the waveguides is set to obtain a  $180^\circ$  phase shifter for the most basic unit cell, which gives a more constant phase shift over the frequency range. The waveguides have been selected to have a length of 8 unit cells plus some transitions for impedance matching between reference CLAF-SIW and the CLAF-SIW with phase-shifting elements. To appropriately measure the phase shifter prototypes in CLAF-SIW,

some transitions from coaxial cables connected to the vector network analyzer (VNA) to this waveguide type are needed. In Fig. 4(a), it is shown a transition between grounded coplanar waveguide (GCPW) and AF-SIW (going through SIW, joining two types of transition). The geometrical parameters of the above transitions are specified in the caption of Fig. 4, and their S-parameters are displayed in Fig. 4(b). Both transitions are based on [25] and [26], respectively. As the authors show, these are wideband transitions due to the progressive modification of the waveguide widths. A return loss lower than  $-15$  dB with a good transmission level is achieved from 31 GHz to 50 GHz.

Another problem to be solved is the reduction of reflections when connecting the reference CLAF-SIW to the waveguide section loaded with SIH elements. These phase-shifting elements in the CLAF-SIW modify the impedance of the waveguide so that a slight reflection may occur. To design these transitions, it has been used unit cells that have SIH whose sizes progressively scaled from zero (no SIH) to the designed size of the SIH that composes the CLAF-SIW phase shifter. This approach to design transitions has also been employed in other loaded waveguides [24, 27]. Each CLAF-SIW phase shifter has its own transition since it depends on the phase-shifting element selected to load the CLAF-SIW (see Fig. 5(a)). As an example, Fig. 4(c) presents the design through two unit cells of simple SIH sizes. A good transition from an empty CLAF-SIW to a CLAF-SIW with phase-shifting elements can be obtained by introducing additional SIH elements that progressively vary in size. Fig. 4(d) presents the S-parameters of a back-to-back design in CLAF-SIW, where the transition based on phase-shifting elements is used at both ends of the loaded CLAF-SIW. The simulated results reveal an improvement in the  $|S_{11}|$  achieving  $-15$  dB approximately from 31.9 GHz to the end of the band ( $-20$  dB from 33.6 GHz).

## 3. Experimental validation and discussion

Several phase shifters in CLAF-SIW are manufactured to validate the proposed designs. Fig. 5(a) shows the layers that form the prototype, and Fig. 5(b) illustrates the way to assemble these layers to obtain a phase shifter in CLAF-SIW. These shown layers are the middle and bottom ones of the phase shifter. Indeed, the intermediate layer has the transitions and EBG unit cells detailed in 2.3 and 2.1, respectively. In the bottom layer (and the top layer, which is not shown), the phase-shifting elements presented and analyzed in 2.2 are implemented. For the sake of completeness, the case of the design with simple SIH cavity unit cells has been considered in both glide-symmetric and mirror-symmetric configurations.

The measured performances of the fabricated phase shifters are shown in Figs. 6(a)-6(b), which display the  $|S_{11}|$  and  $|S_{21}|$  simulated and measured results. Agreement for measured and simulated reflection and transmission values are observed in all CLAF-SIW prototypes in the frequency range from 30 to 50 GHz. The impedance bandwidth, where

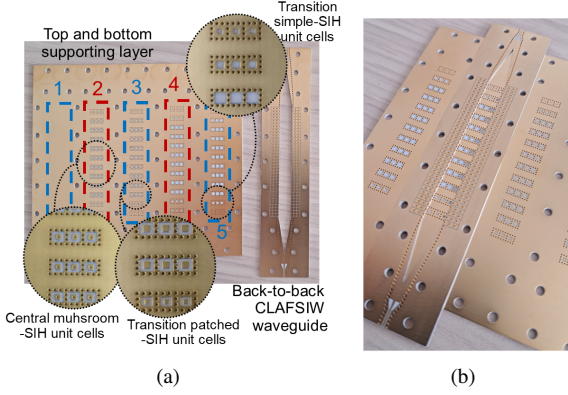


**Figure 5:** Fabricated phase shifters in CLAF-SIW: (a) Unassembled layers where in the top/bottom layer are implemented: “1” reference waveguide, “2” waveguide with SIH and mushrooms in glide symmetry, “3” waveguide with SIH and patches in glide symmetry, “4” waveguide with simple SIH in mirror symmetry and, “5” waveguide with simple SIH in glide symmetry. Zoom of different zones are realized: zone of central mushroom-SIH unit cells, zone of transition patched-SIH unit cells, and transition simple-SIH unit cells (Fig. 4(c)). (b) Example of an assembled phase shifter (top layer is not shown).

the  $|S_{11}|$  is below -10 dB, covers the 30.9 GHz to 50 GHz frequency range (a relative bandwidth of 47.2%) for the reference CLAF-SIW. The impedance bandwidth for each phase shifter is limited by the lower frequency, from 30.8 GHz for the one with SIH elements, from 31.3 GHz for the one with patched-SIH elements, and 32.2 GHz for the one with mushroom-SIH elements. However, the devices are limited by losses due to increased cut-off frequencies and leakage at transitions, which are due to the gaps between laminates. The maximum losses for the reference CLAF-SIW are 0.2 dB in simulation and 1.5 dB in measurement from 33 GHz. The phase shifters have maximum losses of 2.1 dB from 33 GHz for the one with SIH elements, 2.4 dB from 31.8 GHz for the one with patched-SIH elements, and 2.3 dB from 34.1 GHz for the one with mushroom-SIH elements. It is noted that the  $|S_{11}|$  is limited by the GCPW-SIW transition. It is important to note that the transmission level is mainly affected by the connectors, the field leakage produced by the undesired gap in the SIW to AF-SIW transitions, and their dielectric losses. This is currently inherent in the technology, and when optimal transitions are designed to consider gaps, prototypes would have reduced losses. The gap effect can be observed in the increase of the cut-off frequency for all the measurements. However, in this way, it is possible to study the gap produced in this type of structure, estimated at 0.015 mm. The mirror-symmetric prototype demonstrates the stopband (Fig. 6(c)) against the other prototypes [15, 18].

The simulated and measured phase shift is shown in Fig. 6(f). A high correlation between the simulations and the measurements can be observed. It is possible to notice how the phase shifter with simple SIH achieves a quasi-planar

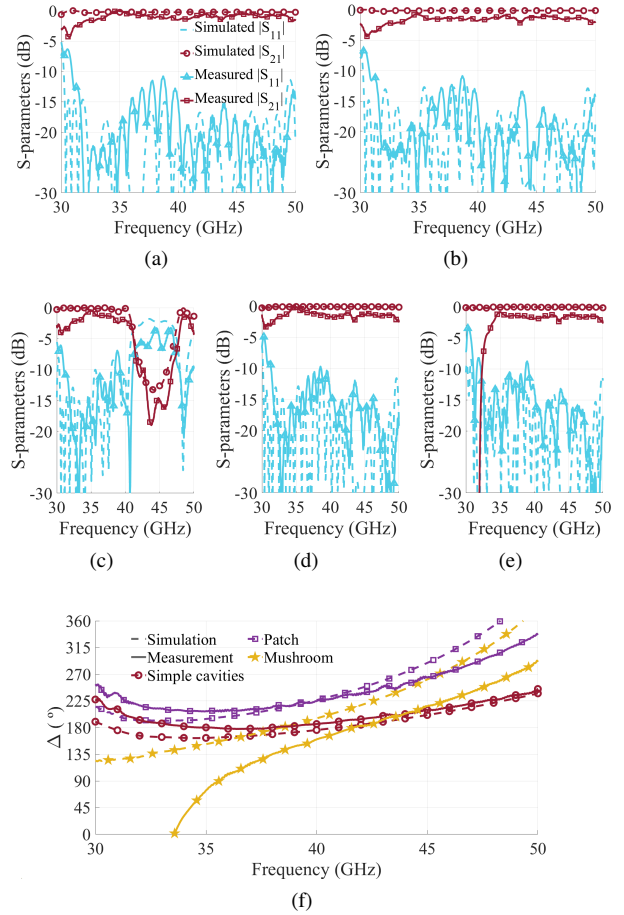


**Figure 6:** Simulated and measured results of the prototypes. S-parameters of the phase shifters indicated in Fig. 5(a) as: (a) “1” reference waveguide, (b) “5” glide-symmetric SIH, (c) “4” mirror-symmetric SIH, (d) “3” patch-SIH, and (e) “2” mushroom-SIH. The legend is common in the subfigures (a)-(e). (f) Phase shift.

phase shift of  $187^\circ \pm 10.4^\circ$  in the frequency range between 31.6 GHz and 42.9 GHz (30.3% relative bandwidth). The phase shifter based on SIH with patches allows a less constant phase shift and a higher value than in the simulation due to expected dispersion, for which at 40 GHz, the phase shift is  $224.6^\circ$ . The phase shifter based on the SIH with mushrooms has the same frequency phase shift slope as in the simulation, but the value at the starting frequency is smaller. At 37 GHz, the phase shift is  $119.8^\circ$ , and it increases to  $216.1^\circ$  at 45 GHz (a slope of  $12^\circ/\text{GHz}$ , which matches the simulated value for a unit cell by the number of unit cells included). The discrepancies result from the gap and manufacturing tolerances, and that is more prominent at low frequencies where the gap and manufacturing tolerances produce modifications in cut-off frequencies for more complex designs such as those based on mushrooms.

Table I is provided to compare this work at mm-waves with others based on the PCB-manufacturing process. The works in [11], [12], and [28] achieve phase shifter designs in AF-SIW technology by including some dielectric parts

**Table 1**  
Comparison between related works

Ref.	Technology	Freq. range (GHz)*	Phase over freq.	IL (dB) <sup>†</sup>	Compactness (°/mm)
[11]	AF-SIW	31.5-35.6	constant	0.52	9.0
[12]	AF-SIW	26-40	constant	3.20	5.7
[28]	AF-SIW	27-37	constant	0.58	10.7
[29]	E-SIW	26-40	constant	1.59	8.91
[30]	E-SIW	26-40	constant	1.9	8.3
This work	CLAF-SIW	31.6-42.9	constant	2.1 <sup>1</sup>	5.1
		37.7-41.8	const./linear	2.4 <sup>2</sup>	6.4
		Not appl.	linear	2.3 <sup>3</sup>	Not appl.

\*Operating bandwidth in terms of the phase-shifting (with a phase-error of 2.5° each 45° of phase shift).

<sup>†</sup>IL: Maximum insertion losses. Reference CLAF-SIW: 1.5 dB from 33 GHz, <sup>1</sup>from 33 GHz, <sup>2</sup>From 31.8 GHz, <sup>3</sup>from 34.1 GHz.

which modify the effective waveguide width. The characteristics vary in bandwidth and compactness. Other works, such as [29] and [30], focus on the E-SIW technology; the phase shift is produced by using microstrip lines of different lengths on the ends of the E-SIW or by the direct modification of the waveguide width, respectively. Unlike the previous works, we propose using periodic structures in CLAF-SIW to obtain different phase shift behaviors over frequency. The phase shifter based on SIH unit cells achieves a constant phase shift over a wide bandwidth, comparable to previous works' performance. The phase shifter that employs SIH with mushroom unit cells allows linear phase shift behavior over the frequency. The phase shifter composed of SIH with patches combines both behaviors in different frequency ranges with higher values of phase shift. It should be noted that none of the previous technologies have achieved phase shifters other than the constant phase shift function over a large bandwidth. In some devices, it is interesting to compensate and change this value with frequency [17]. The insertion losses shown in Table I correspond to the measured results. It should be noted that the insertion losses are slightly higher in the proposed phase shifters. This is due to the PCB material, transitions, and assembly tolerances. In the case of the works in AF-SIW that use similar transitions and have lower losses, the PCB used is Rogers RT/Duroid 6002, whose  $\tan\delta$  is 0.0012 (at 10GHz), slightly less than half that of the dielectric used in this work. However, most of the losses in this work are estimated to be leakage losses in the AF-SIW transitions. This is due to the considerable length and possible gaps in the transitions. The referenced works allow reduced losses by welding the laminates together or having more control over the assembly with higher screw density.

#### 4. Conclusion

This paper proposes some unit cell designs in CLAF-SIW to introduce phase shifts in this waveguide technology. The propagation zone of the CLAF-SIW is exploited to introduce phase-shifting elements on the bottom and top layers. These elements are based on SIH, and glide-symmetry is used in the periodic unit cells to mitigate their dispersion. Simple SIH, patches over SIH, and mushrooms inside SIH have been analyzed as phase-shifting elements.

Several prototypes have been manufactured to validate the proposed phase shifter designs in CLAF-SIW. The measurements have indicated that the prototype performs in the 33 GHz to 50 GHz frequency range with a  $|S_{11}|$  below -10 dB and  $|S_{21}|$  above -2.4 dB, except the mushroom-SIH phase shifter for which the issue is known. The obtained phase shift depends on the unit cell, resulting in different phase shift behavior over the frequency. The simple SIH unit cell achieves a constant phase shift of around 180° over a wide range, patches over the SIH can increase the phase shift with several behaviors, and mushrooms inside the SIH allow linear phase shift with frequency. The slight discrepancies in the phase shift observed between measurements and simulations are due to gaps and manufacturing tolerances. The insertion losses will be easily reduced in the future with the design of optimal transitions for this technology since they are mostly due to leakage losses. The presented CLAF-SIW phase shifter designs, whose phase behavior can be adjusted in frequency, may have application, for example, in devices where: i) a phase compensation at their outputs is needed (as is the case of beamforming networks or Doherty amplifier [17]), ii) a determined phase constant behavior over the frequency is required for a target radiated direction in leaky-wave antennas or iii) to introduce a stable phase shift at one of the power divider outputs (needed in the feeding of monopulse antennas).

#### Acknowledgment

This work has been supported by grant TED2021-129938B-I00 funded by MCIN/AEI/10.13039/501100011033 and by the European Union NextGenerationEU/PRTR. It has also been supported by Grants PID2020-112545RB-C54, PDC2022-133900-I00, and PDC2023-145862-I00, funded by MCIN/AEI/10.13039/501100011033 and by the European Union NextGenerationEU/PRTR. It has also been supported by Grant FPU20/00256 funded by MICIU/AEI/10.13039/501100011033 and by ESF Investing in your future. It is also part of Programa Margarita Salas, from the European Union NextGenerationEU and Ministerio de Universidades (Gobierno de España), and part of Contract SAD 22006912 (SuMeRIO) of Brittany Region. Funding for open access charge: Universidad de Málaga / CBUA.

#### References

- [1] D. Deslandes, K. Wu, Single-substrate integration technique of planar circuits and waveguide filters, *IEEE Transactions on Microwave Theory and Techniques* 51 (2003) 593–596.
- [2] K. Wu, M. Bozzi, N. J. Fonseca, Substrate integrated transmission lines: Review and applications, *IEEE Journal of Microwaves* 1 (2021) 345–363.
- [3] D. Deslandes, K. Wu, Accurate modeling, wave mechanisms, and design considerations of a substrate integrated waveguide, *IEEE Transactions on Microwave Theory and Techniques* 54 (2006) 2516–2526.
- [4] E. Rajo-Iglesias, M. Ferrando-Rocher, A. U. Zaman, Gap waveguide technology for millimeter-wave antenna systems, *IEEE Communications Magazine* 56 (2018) 14–20.

- [5] F. Parment, A. Ghiotto, T.-P. Vuong, J.-M. Duchamp, K. Wu, Air-filled substrate integrated waveguide for low-loss and high power-handling millimeter-wave substrate integrated circuits, *IEEE Transactions on Microwave Theory and Techniques* 63 (2015) 1228–1238.
- [6] A. Belenguer, H. Esteban, A. L. Borja, V. E. Boria, Empty SIW technologies: A major step toward realizing low-cost and low-loss microwave circuits, *IEEE Microwave Magazine* 20 (2019) 24–45.
- [7] P.-S. Kildal, E. Alfonso, A. Valero-Nogueira, E. Rajo-Iglesias, Local metamaterial-based waveguides in gaps between parallel metal plates, *IEEE Antennas and Wireless Propagation Letters* 8 (2008) 84–87.
- [8] M. J. Chashmi, P. Rezaei, A. H. Haghparast, D. Zarifi, Dual circular polarization  $2 \times 2$  slot array antenna based on printed ridge gap waveguide technology in Ka band, *AEU-International Journal of Electronics and Communications* 157 (2022) 154433.
- [9] N. Bayat-Makou, A. A. Kishk, Contactless air-filled substrate integrated waveguide, *IEEE Transactions on Microwave Theory and Techniques* 66 (2018) 2928–2935.
- [10] Y. Cao, Y. Cai, L. Wang, Z. Qian, L. Zhu, A review of substrate integrated waveguide end-fire antennas, *IEEE Access* 6 (2018) 66243–66253.
- [11] F. Parment, A. Ghiotto, T.-P. Vuong, J.-M. Duchamp, K. Wu, Double dielectric slab-loaded air-filled SIW phase shifters for high-performance millimeter-wave integration, *IEEE Transactions on Microwave Theory and Techniques* 64 (2016) 2833–2842.
- [12] N.-H. Nguyen, A. Ghiotto, T.-P. Vuong, A. Vilcot, F. Parment, K. Wu, Slab air-filled substrate integrated waveguide, in: 2018 IEEE/MTT-S International Microwave Symposium-IMS, IEEE, 2018, pp. 312–315.
- [13] I. Casero, J. A. Ballesteros, M. D. Fernandez, D. Herraiz, A. Belenguer, Easy-to-assemble and high quality-factor ESIW filter with post-based soldered inverters in X-band, *AEU-International Journal of Electronics and Communications* 142 (2021) 153987.
- [14] A. Araghi, M. Khalily, P. Xiao, R. Tafazolli, D. R. Jackson, Long slot mmwave low-SLL periodic-modulated leaky-wave antenna based on empty SIW, *IEEE Transactions on Antennas and Propagation* 70 (2021) 1857–1868.
- [15] Á. Palomares-Caballero, A. Alex-Amor, P. Padilla, J. F. Valenzuela-Valdés, Dispersion and filtering properties of rectangular waveguides loaded with holey structures, *IEEE Transactions on Microwave Theory and Techniques* 68 (2020) 5132–5144.
- [16] O. Zetterstrom, R. Hamarneh, O. Quevedo-Teruel, Experimental validation of a metasurface luneburg lens antenna implemented with glide-symmetric substrate-integrated holes, *IEEE Antennas and Wireless Propagation Letters* 20 (2021) 698–702.
- [17] Y. F. Pan, Y. Yang, W. S. Chan, S. Y. Zheng, W. Shang, A simple and universal phase control method for designing directional couplers with adjustable phase difference slope and high linearity, *IEEE Transactions on Microwave Theory and Techniques* 71 (2023) 3882–3895.
- [18] C. Segura-Gómez, Á. Palomares-Caballero, A. Alex-Amor, C. Molero, P. Padilla, Air-siw unit cell with glide-symmetric structures, in: 2023 17th European Conference on Antennas and Propagation (EuCAP), IEEE, 2023, pp. 1–4.
- [19] F. Ghasemifard, F. Mesa, G. Valerio, O. Quevedo-Teruel, Propagation characteristics in substrate integrated holey metasurfaces, in: 2020 14th European Conference on Antennas and Propagation (EuCAP), IEEE, 2020, pp. 1–4.
- [20] H. Raza, J. Yang, P.-S. Kildal, E. A. Alós, Microstrip-ridge gap waveguide—study of losses, bends, and transition to WR-15, *IEEE Transactions on Microwave Theory and Techniques* 62 (2014) 1943–1952.
- [21] X.-F. Zhao, J.-Y. Deng, J.-Y. Yin, D. Sun, L.-X. Guo, X.-H. Ma, Y. Hao, Novel suspended-line gap waveguide packaged with stacked-mushroom-EBG structures, *IEEE Transactions on Microwave Theory and Techniques* 69 (2021) 2447–2457.
- [22] Rajo-Iglesias, Eva and Inclán-Sánchez, Luis and Vázquez-Roy, José-Luis and García-Muñoz, Enrique, Size reduction of mushroom-type EBG surfaces by using edge-located vias, *IEEE Microwave and Wireless Components Letters* 17 (2007) 670–672.
- [23] Pozar, David M, *Microwave Engineering: Theory and Techniques*, John Wiley & Sons, 2021.
- [24] Palomares-Caballero, Angel and Alex-Amor, Antonio and Padilla, Pablo and Luna, Francisco and Valenzuela-Valdes, Juan, Compact and low-loss V-band waveguide phase shifter based on glide-symmetric pin configuration, *IEEE Access* 7 (2019) 31297–31304.
- [25] R. Kazemi, A. E. Fathy, S. Yang, R. A. Sadeghzadeh, Development of an ultra wide band GCPW to SIW transition, in: 2012 IEEE Radio and Wireless Symposium, 2012, pp. 171–174. doi:10.1109/RWS.2012.6175308.
- [26] F. Parment, A. Ghiotto, T.-P. Vuong, J.-M. Duchamp, K. Wu, Broad-band transition from dielectric-filled to air-filled substrate integrated waveguide for low loss and high power handling millimeter-wave substrate integrated circuits, in: 2014 IEEE MTT-S International Microwave Symposium (IMS2014), IEEE, 2014, pp. 1–3.
- [27] Monje-Real, Alberto and Fonseca, NJG and Zetterstrom, O and Pucci, E and Quevedo-Teruel, Oscar, Holey glide-symmetric filters for 5G at millimeter-wave frequencies, *IEEE Microwave and Wireless Components Letters* 30 (2019) 31–34.
- [28] N.-H. Nguyen, A. Ghiotto, T. Martin, A. Vilcot, K. Wu, T.-P. Vuong, A  $90^\circ$  self-compensating slab air-filled substrate integrated waveguide phase shifter, in: 2019 IEEE MTT-S International Microwave Symposium (IMS), IEEE, 2019, pp. 580–583.
- [29] H. Peng, Y. Wu, Y. Zuo, J. Dong, S. O. Tatu, Y. Liu, T. Yang, Synthesis design of equal-length phase shifter based on substrate integrated waveguide and microstrip line, *International Journal of RF and Microwave Computer-Aided Engineering* 31 (2021) e22544.
- [30] H. Peng, F. Zhao, J. Dong, Y. Liu, S. O. Tatu, T. Yang, H. Jin, 3-D empty substrate integrated waveguide phase shifter with equal length, *IEICE Electronics Express* 16 (2019) 20190619–20190619.